RSC Advances

ROYAL SOCIETY OF CHEMISTRY

www.rsc.org/advances

Journal Name

ARTICLE

In-Situ SeO_2 Promoted Synthesis of CdSe/PPy and Se/PPy Nanocomposites and their Utility in Optical Sensing for Detection of Hg^{2+} Ions

Received 00th January 20xx,
Accepted 00th January 20xx

DOI: 10.1039/x0xx00000x

www.rsc.org/

Pawan K. Khanna[a]*, Sreenu Bhanoth[a], Vaishali Dhanwe[a], Anuraj Kshirsagar[a] and Priyesh More[a]

Avoiding use of any external oxidising agent and initiator for the polymerisation process, pyrrole was successfully polymerised to polypyrrole (PPy) using SeO_2 as an internal oxidant which leads to the *in-situ* synthesis of selenium and cadmium selenide polypyrrole (Se/PPy and CdSe/PPy) nanocomposites by chemical and microwave methods. PPy formation during the reaction was monitored by UV-Visible absorption spectroscopy. XRD measurement indicated formation of CdSe/PPy and Se/PPy confirmed nanocomposites. SEM images showed the aggregation of small particles in the form of large globules with smooth surface. HRTEM images revealed the presence of spherical CdSe and Se nanoparticles homogeneously embedded in polypyrrole matrix with interplanar distances of 0.35 nm and 0.4 nm for (111) and (100) atomic planes respectively. As-synthesized CdSe/PPy and Se/PPy nanocomposites were tested for the detection of heavy metal ions. CdSe/PPy and Se/PPy successfully detected mercury ions at 25, 50 and 100 ppm. This article also describes use of pre-synthesized Se/PPy nanocomposite as precursor for synthesis of CdSe/PPy nanocomposite.

Keywords: Chalcogenides, Polypyrrole, Conducting polymer, Nanocomposites, Microwave.

1. Introduction

Among the conducting polymers, Polypyrrole (PPy) has attracted much attention because of its unique environmental stability, ease of preparation, high electrical conductivity, redox property and use as supporting substrate for various noble metals or metal oxides[1-3]. PPy has potential applications in microelectronics, bio-medical applications, optical sensors, batteries, electro-chromic devices, electronic devices and many other advanced technologies[4-7]. Even though polypyrrole is environmentally stable its less stability in air often imparts adverse effect in high-tech applications. In order to make it more stable with improved chemical and physical properties, chemical doping or incorporation of nanoparticles is preferred. Polypyrrole nanocomposites with nano sized inorganic particles (1-100 nm) shows enhanced optical, mechanical, optoelectronic properties[8-9]. There are several reports describing the synthesis and applications of polypyrrole based nanocomposites using pyrrole or polypyrrole as reducing agent[10-11] for metal ions. Metal/PPy nanocomposites such as silver (Ag), Gold (Au), platinum (Pt), palladium (Pd), ruthenium (Ru) /PPy etc prepared by various methods exhibit improved physical and chemical properties[12-15]. Apart from the conventional methods such nanocomposites can also be prepared by simple, quick and reliable method like microwave (MW) irradiation. In fact there are several reports revealing synthesis of nanocomposites by MW method. Bensebaa *et al* have described synthesis of Pt/PPy nanocomposite for application in catalysis wherein they have proposed Pt/PPy nanocomposite as nanocatalyst for direct methanol fuel cells (DMFC)[14]. Similarly, there is report on the interfacial polymerization of pyrrole by use of silver nitrate employing microwave energy leading to formation of Ag/PPy. Polypyrrole nanocomposite with gold nano-particles has been reported by Bertino *et al* wherein a simple and convenient method for controlling of morphology of gold nano-particles and overall nanocomposite is discussed[12]. Metal/PPy nanocomposites have been documented to be useful in wide range of applications such as conducting polymer modified electrodes[16-18] e.g. higher electrocatalytic activity for platinum modified polyaniline/pyrrole dithiophene electrode was reported as compared to that of bulk platinum electrodes and therefore, Pt/PANI or Pt/PPy dithiophene can easily oxidize methanol, hydrogen and C1 molecules. Other notable applications of Metal/PPy nanocomposites include gas sensors[19-21], solar cells[22] etc. As per previous reports, experimental parameters such as polymerisation method, type of an oxidant, reaction time and temperature etc play decisive role in obtaining desired properties in final polymer nanocomposites[23]. The synthesis of metal or

[a] *Nanochemistry Lab, Department of Applied Chemistry, Defence Institute of Advanced Technology (DIAT), Ministry of Defence, Govt. of India, Girinagar, Pune-411025, India. *Corresponding author: pawankhanna2002@yahoo.co.in*

Electronic Supplementary Information (ESI) available: FT-IR, Raman and Particle size distribution of CdSe/PPy and Se/PPy nanocomposites synthesised by chemical and microwave method. See DOI: 10.1039/x0xx00000x

semiconductor/PPy nanocomposite with longer reaction time at room temperature or UV-assisted synthesis for longer irradiation may result in excess oxidation of pyrrole or formation of by-products. To overcome such problems, instant polymerisation method employing mild reaction conditions can be practiced. *In-situ* formation of silver (Ag) nanoparticles leading to Ag/PPy nanocomposite was earlier reported by one of us describing the polymerisation of pyrrole driven by silver nanoparticles without using any external oxidising agent[20]. Similarly, we have also reported the synthesis of Pt/PPy nanocomposite *via* reduction of hexachloroplatinic acid by pyrrole followed by simultaneous oxidation of excess pyrrole and its application in liquefied petroleum gas (LPG) sensing with excellent result at relatively low temperature[21]. As mentioned earlier organic conducting polymers have applicability as sustainable materials due to their promising physico-chemical properties while nano sized inorganic semiconductors possesses high charge mobility, high electric constant and thermal stability. The advantage of both materials can be taken by converting them to hybrid nanocomposites[21]. Several chalcogenide based polymer nanocomposites have been reported such as nanocomposites with polyaniline (Se/PANI[23], CdSe/PANI[24], CdS/PANI[25],) with polypyrrole (Se/PPy[26]), with poly (3-hexylthiophene-2,5-diyl) (CdSe/P3HT[27]), with poly(methyl methacrylate) (CdSe/PMMA[28], CdS/PMMA[29]) etc. which have been shown to be very useful in advanced sensor or solar cell applications[30]. Such nanocomposites have their own importance because of applications in particular research area e. g. CdSe doped P3HT or PCMB nanocomposite reported as active layer in heterojunction photovoltaic device describing significantly more photocurrent in a region surrounding the absorption peak of the CdSe nanoparticles (560-660 nm) containing the CdSe/methyl viologen composite when compared to pristine P3HT: PCBM composite containing devices. However, upon increase in the ratio of CdSe to PCMB performance was also found to be increased[27]. Dhyani *et al*[25] reported a novel route for CdS/PANI nanocomposite using electrochemical polymerisation technique for synthesis of Polyaniline-CdS nanocomposite to evaluate for mediator free biosensing application. In order to prove utility of such nanocomposite in sensing, CdS/PANI matrix was utilized for cholesterol sensing in the concentration range of 50 to 500 $mgdL^{-1}$ with good detection limit of 47.8 $mgdL^{-1}$.

The earlier successful synthesis of Ag/PPy and Pt/PPy nanocomposite and their utility in gas sensing application motivated us for the *in-situ* synthesis of Se/PPy and CdSe/PPy nanocomposite. It is noticed from the literature that, there are only few reports on CdSe/PPy nanocomposite. To the best of our knowledge we have not come across *in-situ* synthesis of Se/PPy and CdSe/PPy nanocomposites employing SeO_2 as an internal oxidising agent for polymerisation of pyrrole. Additionally such in-situ SeO_2 promoted reactions have not been described for Se/PPy and CdSe/PPy nanocomposites avoiding use of external oxidants[23,31-33,] although, Selenium dioxide has been employed as a mild oxidizing agent in many organic conversions[34].

Se/PPy and CdSe/PPy nanocomposites like other nanocomposites with conducting polymer have emerged as an important class of the materials for gas sensors, solar cells and other electrical devices[23,26], there is no report describing their utility in heavy metal ion detection. Heavy metal ions have been detected by several class of nanomaterials e.g. gold nanoparticles, QDs based devices, by exchange of cations as well as by use of biosensors etc[35, 36,37]. Polymer nanocomposites have also shown promise for the detection of heavy metal ions e. g. Wang *et al* employed Ag@polyaniline nanocomposite for the detection of mercury ion using surface enhanced Raman scattering (SERS) technique[38]. Nafion/graphene nanocomposite was reported by Jahed *et al* for the detection of Cd^{2+}, Pb^{2+} metal ions[39]. Similarly, Yanhong *et al* have described utility of the polyaniline/graphene nanocomposite for heavy metal ion detection using electrochemical method[40], Water purification from metal ions including heavy metal ions using carbon nanoparticle/polyethylenimine (PEI) was explained by Khaydarov *et al* based on the interaction of metal ions with composite[41]. Many of these techniques require special instrument, tedious metal extraction process, use of radionuclides or conversion of the composite in to special electrodes for the detection of heavy metal ions. However, none of the report explains use of CdSe/PPy nanocomposite solution for the detection of mercury ion at ppm level using UV-Visible spectroscopy which is a simple novel concept. The present article therefore, describes *in-situ* SeO_2 promoted single step chemical as well as microwave synthesis of Se/PPy and CdSe/PPy nanocomposite for part per million (ppm) level detection specific to mercury ions (Hg^{2+}) using UV-Visible absorption spectroscopy. Moreover, we have successfully employed chemically synthesized Se/PPy as a precursor for synthesis of CdSe/PPy nanocomposite.

2. Result and Discussion

2.1 Synthesis and Characterization

Several oxidising agents have been reported for the polymerisation of pyrrole which mostly demands removal of impurities and by-products through workup for obtaining pure polypyrrole. However, for synthesising composites of reactants present in the reaction, it is possible to avoid multistage work up and loss of important ingredients. The present research shows that, CdSe/PPy and Se/PPy nanocomposites can be synthesized by using SeO_2 a mild internal oxidising agent. Such protocol for CdSe/PPy and Se/PPy has never been described and present work is first of its kind for *in-situ* polymerisation of pyrrole. The overall reaction is shown in scheme 1. It is opined that, basic -NH group in pyrrole promotes the dissociation of Se from selenium dioxide to result Se/PPy or CdSe/PPy nanocomposite in presence of cadmium acetate dihydrate.

The whole reaction sequence can be summarised as follows, the presence of selenium dioxide in reaction mixture initiates the oxidative polymerisation process in both cases so as to form polypyrrole (PPy). The oxidizing ability of SeO_2 converts pyrrole to their unstable radical cations through one electron oxidation process. Highly unstable radical cations get

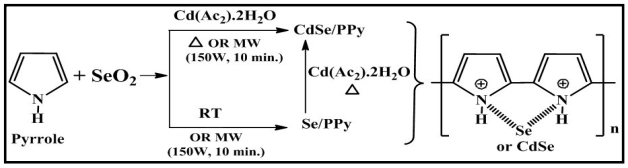

Scheme 1 Synthetic routes for synthesis of CdSe/PPy and Se/PPy nanocomposite *via* polymerization of pyrrole.

stabilized by fusing or combining with each other forming stable long chain of PPy[41]. The overall process takes place *via* well known initiation, propagation and termination steps of the free radical polymerization mechanism. The pictorial mechanism for PPy formation is depicted in scheme 2. During the conversion of Py to PPy, SeO_2 gets reduced to Se^{2+} which further reduces to Se^0 or Se^{2-} ion due to presence of excess pyrrole. Later, the excess pyrrole present in reaction mixture acts as reducing as well as size controlling agent and therefore, nano-sized Se or CdSe particles formation takes place. During such a transformation, nucleation and growth of Se and CdSe nanoparticles were well controlled. Polypyrrole is long chain polymer and therefore, nanoparticles formed in the reaction mixture remains embedded in the polypyrrole network leading to the agglomeration which is also confirmed from SEM images (Fig. 4).

The microwave assisted synthetic method gives desired product in a very short period of time due to highly localised energy present in the system when compared with chemical method. CdSe/PPy & Se/PPy nanocomposites so-synthesized were analyzed by various tools.

The UV-Visible spectra of chemically synthesized CdSe/PPy nanocomposite in DMF showed bands at 445 nm (broad) and 650 nm indicating formation of polypyrrole along with CdSe nanoparticles (Fig.1a). Similarly, UV-Visible absorption spectrum of Se/PPy prepared by chemical method showed peaks at 380, 456 and 609 nm corresponding to absorption due to PPy ring, bipolaron of PPy and Se nanoparticles respectively (Fig.1b). There was however, a little shift in absorption energy when the same reaction was performed under microwave energy. In absorption profile for the microwave assisted reactions, two absorption bands at 440 nm and 600 nm corresponding to PPy and CdSe nanoparticles were obtained for CdSe/PPy whereas Se/PPy showed peaks at 375 nm for PPy and broad featureless absorption at 605 nm for Se nanoparticles (Fig.1d and e).

As has been mentioned in experimental section, Se/PPy can be used as a precursor to synthesize CdSe retaining the matrix. Indeed, we succeeded in isolation of CdSe/PPy nanocomposite with absorption bands at 530 nm tailing into visible region indicating the presence of CdSe nanoparticles (Fig.1c). The shift in absorption values for PPy and CdSe or Se nanoparticles could be due to the difference in particle size, morphology of the inorganic entities as well as their possible interaction with PPy. The band gap energies of CdSe/PPy and Se/PPy nanocomposites synthesized by chemical and microwave method were determined from absorption wavelength and schematic presentation is shown in scheme 2.

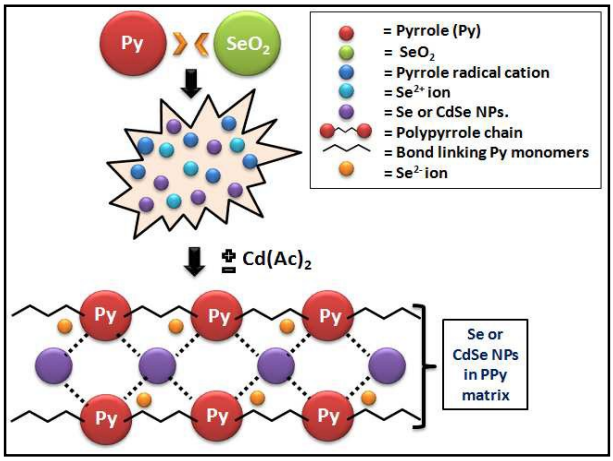

Scheme 2. Possible mechanism of PPy formation *via* radical cation and aggregation of CdSe/Se nanoparticles in PPy matrix.

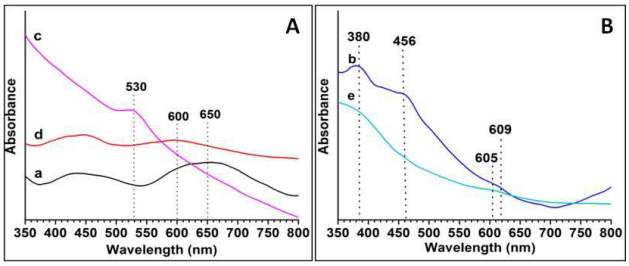

Fig.1 UV-Visible absorption spectra of A) CdSe/PPy synthesized by (a) chemical (d) microwave, (c) using Se/PPy as precursor and B) Se/PPy synthesized by (b) chemical and (e) microwave method.

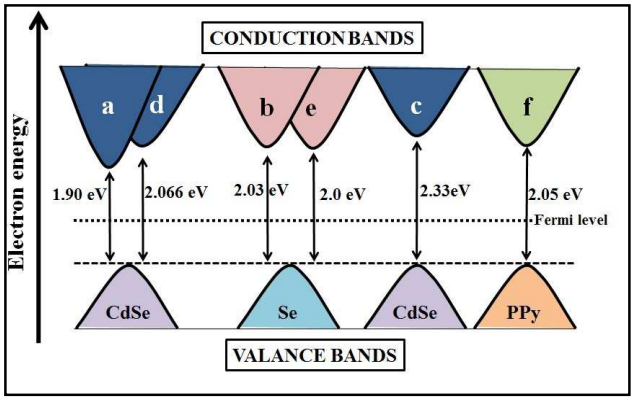

Scheme 3 Schematic representation of band gap energies of CdSe/PPy (a, c, d) and Se/PPy (b, e) nanocomposites as per synthetic methods given in fig.2. f) band gap of PPy (all are not to the scale)

From scheme 3 it can be seen that, The Eg values for CdSe/PPy and Se/PPy nanocomposite synthesized by chemical method were found to be 1.9 and 2.03 eV (scheme 3 a, b) and nanocomposites synthesized by microwave method were 2.06

& 2.04 eV (scheme 3d, e) respectively while CdSe/PPy synthesized *via* Se/PPy as precursor showed band gap energy of 2.33 eV (scheme 3c). These values are higher than the reported values of CdSe (bulk value 1.72 eV)[42] and Se nanoparticles (bulk value ~1.7 eV)[43]. The band gap of polypyrrole has been reported to be 2.05 eV which is also closely reflecting by taking respective absorption wavelength in our samples[44].

The photoluminescence (PL) spectra of the CdSe/PPy and Se/PPy nanocomposites synthesized by both methods were observed with broad emission in the range of 480 nm to 650 nm (Fig.2 A and B). The excitation of CdSe/PPy nanocomposite synthesized by both methods at 450 nm showed emission near 550 nm with slight difference in the intensity as evident from fig. 2A (a, c, d). However, Se/PPy nanocomposites synthesized by chemical method showed emission at 540 nm and that by microwave method at 550 nm as shown in fig. 2B (b) and (e) respectively. The broad emission obtained in all cases can be attributed to the electron-hole recombination phenomena and shallow and deep traps (defects) in the crystal structure.

CdSe is known to have two crystal structures viz, zinc blende (cubic) and wurtzite (Hexagonal). In case of zinc blende, intensity at (111) plane is normally the highest for spherical particles. In the present case, PXRD pattern of CdSe/PPy and Se/PPy showed broad reflections in the region of 23°, which is the characteristic peak of the PPy as shown in Fig 3(A and B). Three peaks obtained in case of CdSe/PPy can be attributed to structure[45]. The sample showed broadened XRD pattern due to presence of nanometer sized CdSe in polypyrrole matrix.

The diffraction for polypyrrole was not so clear possibly due to overlapping of the characteristic PPy peak ($2\theta=23^0$) with (111) plane of CdSe as well as because of excellent crystallinity of CdSe which is evident from good intensity of (111) peak. Absence of diffraction at 2θ $30\text{-}31^0$ implies that CdSe/PPy nanocomposite is free from elemental selenium. The crystallite size calculated using Scherrer equation taking 2θ at (111) plane of CdSe/PPy with FWHM of 3.39^0, resulted in a size domain of 2.40 nm (Fig.3a). The present findings show that, the crystallite size is well correlated with the estimation made from TEM.

(111), (220) and (311) diffractions corresponding to cubic crystal Se/PPy showed the presence of one broad peak with two humps. Shallow merged pattern at about 23^0 can be considered due to PPy however over all broad diffraction profile from $23\text{-}31^0$ indicate formation of selenium nanoparticles in the matrix (fig. 3B). The peaks between $24\text{-}31^0$ and 52^0 were due to (100), (101) and (210) diffractions of Se nanoparticles which matches with reported values for tetragonal crystal structure of elemental selenium[46]. Other low intensity broad peaks in the range of $45\text{-}50^0$ reflect the presence of poorly crystalline (close to amorphous) selenium in polypyrrole matrix. Similar XRD pattern were obtained for Se/PPy and CdSe/PPy synthesized by microwave irradiation method as well as by using Se/PPy as a precursor. CdSe and Se lattice spacing were calculated by employing Bragg's equation

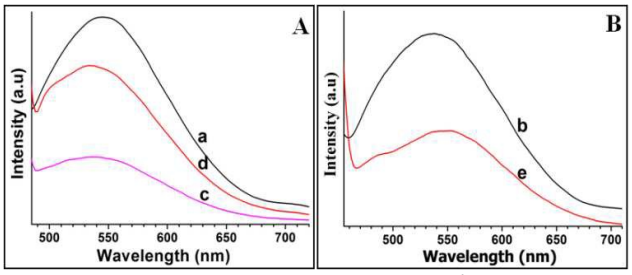

Fig.2 Photoluminescence spectra of A) CdSe/PPy synthesized by (a) chemical (d) microwave, (c) using Se/PPy as precursor and B) Se/PPy synthesized by (b) chemical and (e) microwave method.

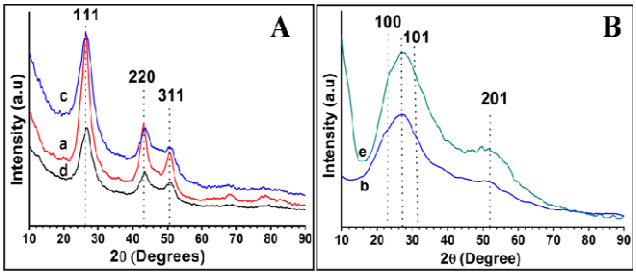

Fig.3 Powder XRD of A) CdSe/PPy synthesized by (a) chemical (d) microwave, (c) using Se/PPy as precursor and B) Se/PPy synthesized by (b) chemical and (e) microwave method.

(1) and was found to be about 0.3422 nm and 0.3862 nm which is very close to that is estimated from HRTEM.

$$n\lambda = 2\,d\sin\theta \qquad (1)$$

Where, n is integer, λ represents the wavelength of incident X-rays, d and θ are spacing between crystal planes and diffraction values respectively.

The presence of polypyrrole in nanocomposite was also confirmed by FTIR. As shown in figure $S1^+$, both CdSe/PPy and Se/PPy showed almost similar spectra with little shift in the peak values due to difference in the interaction of CdSe and Se nanoparticles with nitrogen atom of PPy in the composite. However, red shift obtained for the samples synthesized by microwave method, may be because of greater surface defects generated after irradiation and due to weak interaction between CdSe and Se nanoparticles with nitrogen atom of PPy. Almost all characteristic bands of the PPy were observed in FTIR spectra for both nanocomposites even though they were prepared by different methods. The FTIR peaks for C=C, C=N, N-H, C-H asymmetric and symmetric stretching, C-N stretching, PPy ring, C-H in and out of plane deformations and $C\text{-}N^+\text{-}C$ bipolaron stretching were observed and values of all these vibrations are given in table $S1^+$ which are in close agreement with the reported FTIR values of PPy[47, 48]. It is assumed that, the PPy present in the Se/PPy and CdSe/PPy nanocomposites is doped with Se^{2-} ions. These Se^{2-} ions are bonded with the N^+ atom present in the pyrrole ring. The peaks obtained in the range of 1700-1650 cm^{-1} were due to the backbone oxidation after exposure of PPy to the air[21]. The interaction of inorganic

nano-particles in the present case is evident from the red shift of about 30 cm^{-1} for C=C stretching frequency which was originally at 1562 cm^{-1} for polypyrrole . (Table S1)

The Raman spectra obtained for CdSe/PPy and Se/PPy also shows the characteristic peaks of the PPy as shown in figure S2 A and B[†]. The major peaks obtained in Raman spectra of CdSe/PPy and Se/PPy were assigned to various vibrations of PPy and was in good agreement with the reported values of PPy. The shift in values clearly confirms the presence of nanoparticle and PPy interaction as already stated. The values for b_1 symmetric in plane PPy ring deformation, a_2 symmetric out of plane C-H vibration, a_1 symmetric in plane C-H deformation, b_1 symmetry of N-H stretching vibration, a_1 symmetry of ring vibration and C=C backbone antisymmetric stretching in PPy were observed and values for these vibrations are given in table S1[†][49, 50]. The peak obtained at 398 cm^{-1} in all samples is attributed to the second order spectra of amorphous selenium[51].

The particle size distribution of the CdSe/PPy and Se/PPy nanocomposite was found in the range of ~1-13 nm indicating presence of various sized nanoparticles homogeneously incorporated in polypyrrole matrix (Fig. S3[†]). CdSe and Se nanocomposites synthesized by chemical method showed higher density distribution corresponding to particle size 6 nm and 3 nm (Fig. S3 a,b[†]) respectively. On the other hand in case of CdSe and Se nanocomposites synthesized by microwave irradiation method, higher density distribution corresponding to smaller size particle in the range of 3-4 nm indicating narrow distribution as compared with chemical method (Fig. S3d,e[†]). However, CdSe/PPy synthesized using Se/PPy as precursor showed wide particle size distribution with higher density distribution corresponding to 4 nm (Fig. S3c[†]). If the temperature and time of reaction is increased CdSe and Se nanoparticles could undergo further ripening leading to larger sized particles[21]. Furthermore, the particle size obtained from TEM images also in good agreement with the results obtained from particle size analyser.

The morphology and surface properties of CdSe/PPy, Se/PPy and existence of CdSe, Se nanoparticles in PPy matrix were confirmed by Scanning Electron Microscopy (SEM) and Energy Dispersive X-ray analysis (EDAX) (Fig. 4 and 5). SEM images of CdSe/PPy and Se/ PPy synthesized by both chemical and microwave method reveal the aggregation of small particles in the form of large globules with smooth/rough surface. From SEM images (Fig. 4a and d), CdSe/PPy synthesized by chemical and microwave method shows same morphology since there was lot of agglomeration leading to the formation of larger globules with rough surface. It was very difficult to identify or comment on the size of the CdSe nanoparticles from SEM images because of the agglomeration. However, smaller particles on the surface of the large globules can be easily identified. CdSe/PPy synthesized via Se/PPy precursor route shows irregular and bulky/clumsy morphology of nanocomposite. In case of the SEM images obtained for Se/PPy synthesized *via* chemical and microwave methods (Fig. 4b and e), comparatively smaller but smooth globules are observed. The surface of these globules was too smooth so that, the presence of nanoparticles from the images can not be identified easily. The EDAX, XRD results and TEM images obtained for the nanocomposite also confirming the presence of respective nanoparticles in PPy network.

The EDAX analysis of nanocomposites synthesized by chemical and microwave method confirms the presence of CdSe and Se nanoparticles in polypyrrole matrix with near stoichiometric ratio (Fig. 5).

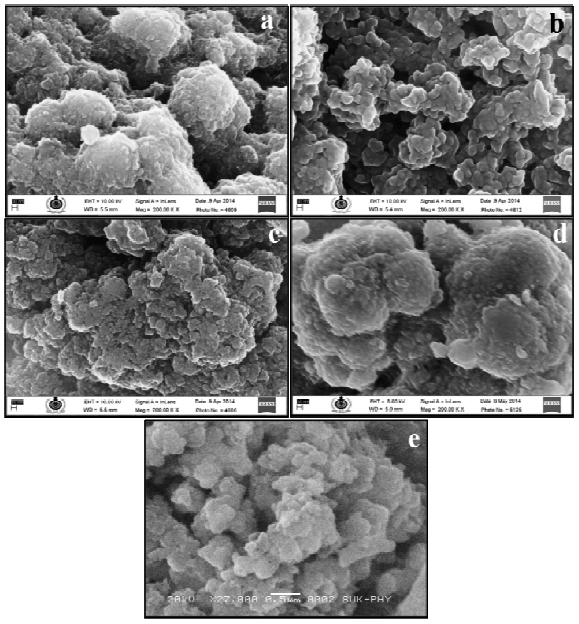

Fig.4 SEM images of CdSe/PPy and Se/PPy synthesized by (a, b) chemical method (d, e) microwave method respectively and (c) CdSe/PPy synthesized by using Se/PPy as precursor. Scale bar is 30 nm for images (a, b, c, d) and 500 nm for image (e).

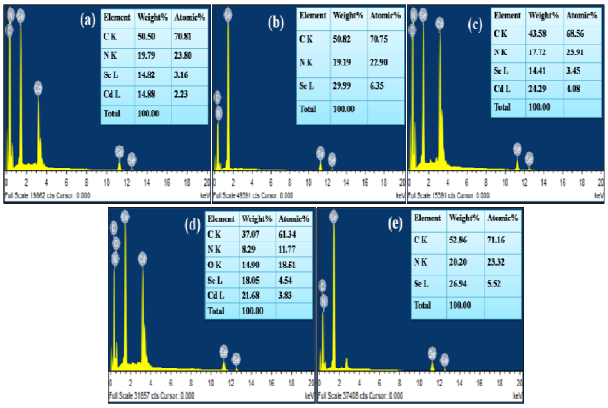

Fig.5 EDAX of (a) CdSe/PPy and (b)Se/PPy synthesized by chemical method, c) CdSe/PPy synthesized by using Se/PPy precursor (d) CdSe/PPy and (e) Se/PPy synthesized by microwave method.

The near 1:1 ratio obtained for CdSe indicating purity of sample prepared by chemical method (fig 5a) however, the sample that was synthesized by microwave method showed presence of oxygen as well as excess cadmium thereby indicating microwave method yielded cadmium rich nanocomposite (Fig. 5d). The oxygen penetration during the work-up might be due to possible leaching of composite making it a little porous which will then have possibility of trapping oxygen during the reaction or during work-up.
Similarly non-stoichiometric CdSe/PPy composite from Se/PPy precursor could be due to absence of required selenium elimination from the polymer as well as trapping of unreacted cadmium ions in the polymer matrix (Fig. 5c).

High Resolution Transmission Electron Microscopy (HRTEM) images of CdSe/PPy and Se/PPy nanocomposite are shown in fig. 6. HRTEM images further confirm the presence of nano sized spherical CdSe and Se nanoparticles homogeneously embedded in polypyrrole matrix. Clear lattice fringes observed for CdSe/PPy and Se/PPy nanocomposites synthesized by chemical and microwave irradiation method, indicate the measured interplanar distances of 0.35 nm and 0.4 nm corresponding to (111) and (100) atomic planes respectively which is well supported by XRD pattern shown in Fig. 3 and SAED pattern shown in the inset of fig.6 d and e.

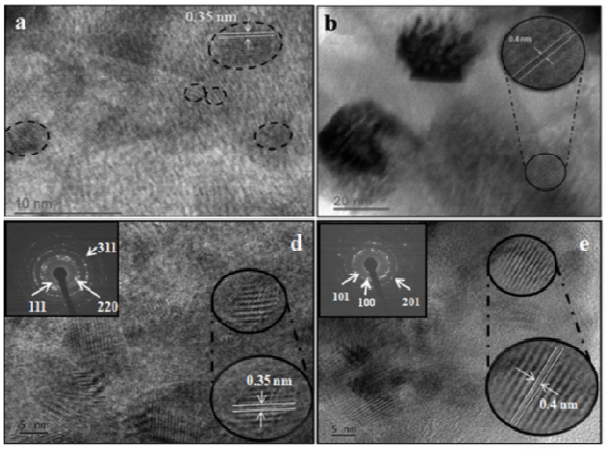

Fig.6 HRTEM images of CdSe/PPy and Se/PPy synthesized by (a, b) chemical method and (d, e) microwave method. Inset of d and e shows SAED pattern for CdSe/PPy and Se/PPy nanocomposites.

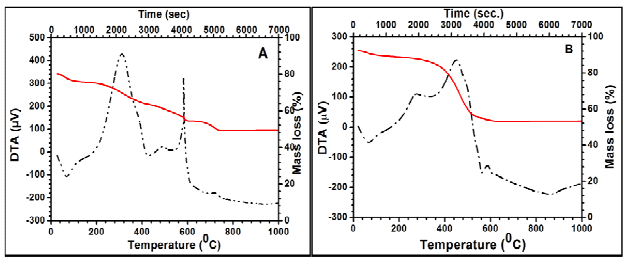

Fig.7 DTA-TGA spectra of (A) CdSe/PPy and (B) Se/PPy synthesized by chemical method.

SAED pattern of CdSe/PPy shows three dark circles corresponding to (111), (220), (311) crystal plane which well matches with PXRD pattern and confirms the high crystallinity. While the diffraction of Se/PPy nanocomposite at (100), (101) and (201) planes shows amorphous nature which is also evident from PXRD.

Thermal stability of CdSe/PPy and Se/PPy nanocomposites were studied by TGA and DSC. Figure 7 shows the thermal decomposition of CdSe/PPy and Se/PPy nanocomposite. It can be seen that, the initial percent weight (%wt) loss near 100^0C in both samples was due to the presence of trace amount of absorbed moisture from environmental exposure. The second stage decomposition from 200-270^0C can be due to degradation of PPy itself as similar observation have been reported by other also[52].The maximum %wt loss (11%) in case of CdSe/PPy was found to be at 410^0C which may be due to further decomposition of PPy and vaporization of selenium from CdSe. The %wt loss at 560^0C will still be possible from PPy for its complete decomposition however %wt loss at 710^0C can be attributed to disintegration of CdSe nanoparticles. In case of Se/PPy nanocomposite maximum (13%) wt. loss observed at 530^0C which can similarly be due to decomposition of Se/PPy nanocomposite. As per previous report Se nanoparticle evaporation takes place at about 440^0C[53] but shift in vaporization temperature can be considered due to the presence of the polymer along with selenium nanoparticles in the present case. Differential Thermal Analysis (DTA) was also studied for the CdSe/PPy and Se/PPy nanocomposites which show step wise exothermic peaks indicating positive enthalpy change due to degradation of composites as observed in TGA studies.

2.2 Impedance analysis

Dielectric studies of the chemically synthesized CdSe/PPy and Se/PPy samples were performed to understand the electrical properties by measuring real part of complex permittivity (Fig. 8). The complex dielectric permittivity (ε^*) is expressed by equation (2),

$$Z^* = Z' - j\,Z'' = 1/j\,C_0\,(Z' + j\,Z'') \qquad (2)$$

Where $C_o = Z_0$ A/d is the empty cell capacitance, Z_0 is the permittivity of the vacuum (8.854×10^{-12} Fm^{-1}), A is the area of the sample and d is the thickness of the sample. Z′ and Z″ are the real and imaginary parts of the impedance. As shown in fig 8(A), increases in permittivity with temperature for both samples suggest semiconducting nature. CdSe/PPy when subjected to impedance analysis showed significant increase in permittivity in the temperature range of (-)25°C to (+)90°C whereas Se/PPy nanocomposite showed only marginal increase. The increase in permittivity can be explained in terms of polarization effect induced in CdSe/PPy because of charge carrier accumulation at the interfaces between CdSe and PPy. It has been reported that, semiconducting particles possibly enhance the temperature dependent polarization due to charge carrier mobility[54]. Since CdSe is a semiconducting

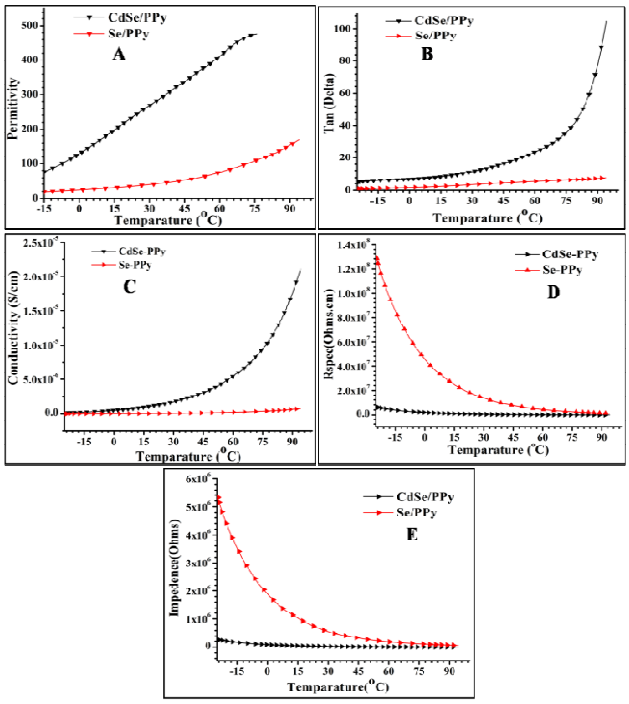

Fig.8 A) Permittivity, B) Dielectric loss tangent C) Conductivity D) Specific resistance and E) Impedance of CdSe/PPy and Se/PPy synthesized by chemical method.

material, it is opined that the polarization may result with increase in charge carrier mobility with temperature thus increases permittivity. Similarly, since the increase in the dielectric loss is due to the increase in charge mobility (conductivity) with the temperature, the dielectric loss tangent increased in case of CdSe/PPy however it remained almost constant in case of Se/PPy (Fig. 8 B). With support of the dielectric studies, **ac** conductivity of the samples was investigated which suggest the typical semiconducting nature with increase in temperature (Fig. 8 C). The **ac** conductivity is expressed as $\sigma_{ac} = \varepsilon_o \omega \varepsilon''$. The enhanced conductivity of CdSe/PPy with increase in temperature can be related to the charge transport properties viz; thermo-ionic emissions and tunnelling of charge carriers[55]. The **ac** conductivity of the Se/PPy is almost constant with increase in temperature, thus suggesting typical insulating characteristics. The insulating nature of Se/PPy can also be confirmed by considering the change in the specific resistance and impedance with temperature (Fig. 8 D and E). The gradual decrease in specific resistance and impedance in case of Se/PPy as compared to CdSe/PPy clearly confirms the insulating characteristics of Se/PPy nanocomposite[56]. In view of poor electrical properties such composites could not be considered for resistive type sensor application. It is indeed desired in modern day research to explore relevance of new materials in useful applications. We therefore, decided to test such composite solution for detection of toxic elements in water e.g. heavy metals particularly mercury which almost matching physical properties with cadmium.

2.3 Mercury ion detection by CdSe/PPy nanocomposite

Generally, metal/PPy nanocomposites are known for their resistivity based sensor applications due to conducting nature. Alternatively, semiconductor/PPy nanocomposites can be exploited as material for optical sensing due to possibility of altering their optical properties. Similarly, nanomaterials (like CdSe/ZnS core/shell)[57] are used to detect Hg^{2+} ions, the selectivity of CdSe QDs alone to detect Hg^{2+} is much superior to its zinc counterpart[58]. The Zinc based systems (ZnS, ZnSe) can detect Pb, Cd and Hg together at ambient conditions while CdSe selectively detects Hg alone even in presence of Pb and Cd ions. There are other reports where researchers have studied the change in photoluminescence properties of CdSe QDs and CdSe/ZnS core/shell QDs when exposed to Hg^{2+} ions in presence of other cations. However, according to those reports only Hg^{2+} ions were detected satisfactorily among the other heavy metal cations[59]. These results highlighted the significance of CdSe QDs in exclusively detecting Hg^{2+} only. Although, HgSe can be synthesized by cation exchange reaction using CdSe[60], there is no previous report exploiting such exchange reactions using composites for detection of heavy metals in water. Also, it should be noticed that, the cation-exchange mechanism was never mentioned or studied for such detection purposes in any of these previous reports. Theoretically, the driving force for exchanges between two cations can be controlled by the difference in relative electronegativities of participating ions, bond energies of Se–Metal, formation energies of the selenide compounds, lattice energies as well as the solvation energies in the presence of a particular coordinating species. Thus, high selectivity of CdSe towards Hg^{2+} ions and presence of Se^{2-} ions on PPy chains makes this material highly useful for Hg^{2+} detection purposes.

It is proposed that cadmium in CdSe/PPy can be exchanged with another element having matching properties. Similarly, Se^{2-} in Se/PPy may be exploited to react with a cation to form metal chalcogenide thus; the concept has potential for detection of heavy metals, especially Hg^{2+}. In the present study, as-synthesized CdSe/PPy nanocomposite was tested for heavy metal ion detection particularly for mercury ions because of similar oxidation state. Indeed, ppm level detection was possible through the experiment in which few drops of well dispersed 100 ppm CdSe/PPy in DMF was treated with 25, 50 and 100 ppm of mercury (II) chloride aqueous solution (2 ml each). The detection was monitored by UV-Visible spectroscopy where absorption bands of CdSe/PPy before and after mixing with aqueous solution of mercury (II) chloride, was studied (Fig. 9A). The treatment with aqueous $HgCl_2$ solution showed disappearance of characteristic absorption due to CdSe nanoparticles (peak or shoulders) at about 540 nm however, low intensity absorption in the range of about 380 and 450-60 nm due to the presence of PPy, were all unaffected. This indicated specific reaction between CdSe and Hg^{2+} ions. HgSe nano-particles may form on the surface during

such dilute testing reactions and will influence the optical behaviour of CdSe nanoparticles. If however the entire cation exchange reaction completes, the band-gap will drastically change and will reach near the band gap of HgSe which is reported to be in the range of 0.4-0.6 eV. This should therefore shift the absorption in the near infra-red range irrespective of possible size quantization effect[61], Such a cationic interchange with ppm level amount of Hg^{2+} ions can be considered an absorption based method for easy detection of Hg. Earlier report suggest the formation of HgSe on the surface and constant red-shift in the absorption and PL spectra for silica coated CdSe quantum dots and its reaction with Hg^{2+} ions[62].

The overall possible chemical reaction for disappearance of characteristic absorption band of CdSe described as in scheme 3. Similarly, as-synthesized Se/PPy nanocomposite was also tested for the mercury ion detection using same procedure using same concentration of mercury (II) chloride. As per the results shown in figure 9B the UV-Visible spectra recorded before and after mixing with $HgCl_2$ solution indicated almost similar profile in absorption spectrum possibly because of release of Se^{2-} ions from Se/PPy for formation of HgSe. Se/PPy therefore, also detects mercury ions from 25, 50 and 100 ppm solution of mercury (II) chloride. Furthermore, as the presence of C-N^+ bond is confirmed by UV-visible spectroscopy and FTIR spectrum (due to presence of Se^{2-} counter ions doping PPy in the process). The doped state of PPy in CdSe/PPy and Se/PPy nanocomposite also plays some role in detection of heavy metal ions as the PPy chains will release the Se^{2-} ions when Hg^{2+} are available in the proximity. For instance, in the present scenario, these bonded Se^{2-} ions would capture the free Hg^{2+} ions to form HgSe molecule. While in case of CdSe/PPy nanocomposite, the mechanism for Hg^{2+} detection is considered through the cation-exchange reaction to form HgSe and the doped PPy will play similar role to further boost Hg^{2+} detection. Therefore, a combination of cation-exchange reaction between the CdSe and the Hg^{2+} ions and release of bonded Se^{2-} ions lead to the formation of HgSe in CdSe/PPy nanocomposite.

In order to extend the scope of CdSe/PPy nanocomposite for detection of other heavy metal ions, experiments were conducted for detection of lead (Pb) ions by the same procedure with various concentrations of Pb^{2+} ions. The treatment of CdSe/PPy for Pb^{2+} ions was found to be unsuccessful and the reason could be the difference between electronegativities[63]. The electronegativity difference of Cd (1.69) and Hg (2.00) is large as compared to Pb (1.87) and Cd. Also, the chlorine ion in $HgCl_2$ salt could play an important role in etching the surface of Cd atoms of CdSe nanoparticles. Since, Chlorine (3.16) is highly electronegative and Cd is more electropositive than Hg, the Cl^- ions will attack the Cd atoms present in the CdSe nanoparticles to form $CdCl_2$ salt. The free Se^{2-} ions from CdSe nanoparticles will then rapidly react with Hg^{2+} ions to produce HgSe particles. Hence, during the cation-exchange reaction, Cd atom in CdSe is easily exchanged with Hg but not with Pb as the electronegativity values of Pb and Cd are relatively similar. For instance, in presence of $PbCl_2$ salt, the CdSe nanoparticles does not show any exchange reaction at optimum conditions. The Cl^- ions in $PbCl_2$ would be reluctant to leave Pb as its electronegativity is relatively similar to Cd.

Additionally, even though Se^{2-} ions are present in the backbone of PPy, they don't react with Pb^{2+} ions. The logical explanation for this will again be similar. The electronegativity of Cl is more than Se^{2-} in PPy ring. Therefore, Pb will prefer chlorine more than Se^{2-} and will not react with Se^{2-} ions which are bonded with N^+ in PPy. Hence, both the nanocomposite (CdSe/Ppy & Se/PPy) fails to detect Pb^{2+} ions but exclusively detects Hg^{2+} ions.

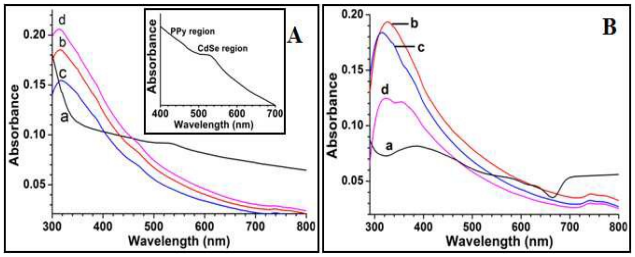

Fig.9 UV-Visible absorption spectra of A) CdSe/PPy and B) Se/PPy showing absorption (a) before and (b, c, d) after mixing with 25, 50 and 100 ppm aqueous solution of $HgCl_2$.

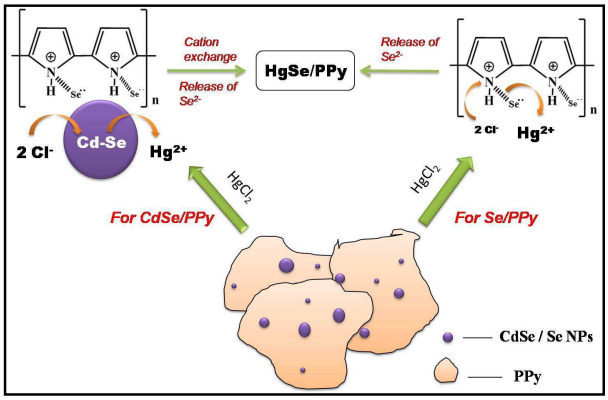

Scheme 3 Possibilities of various reactions during detection of Hg^{2+} ions.

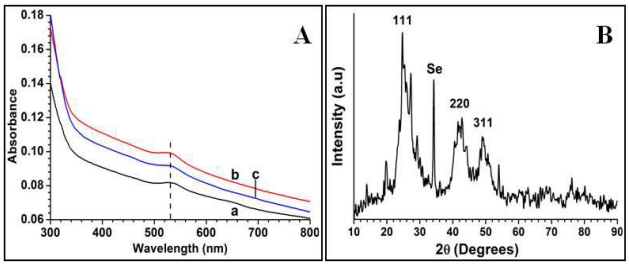

Fig.10 A) UV-Visible absorption of CdSe/PPy and $PbCl_2$ reaction mixture after (a) 1hr (b) 3hrs (c) 12 hrs and B) XRD pattern of CdSe/PPy after reaction with $PbCl_2$

For more clarity, CdSe/PPy was reacted directly with $PbCl_2$ in 1:1 ratio at a larger scale at room temperature and monitored its absorption profile by UV-Visible spectroscopy. Absorption spectra obtained after 1hr, 3hrs and 12 hrs showed no change in UV-Visible absorption of CdSe nanoparticles (Fig. 10A) and the XRD measurement confirmed the final product to be CdSe nanoparticles with diffraction peaks at (111), (220) and (311) as shown in fig.10B. The extra peak obtained in XRD near 32^0 was assigned to the presence of selenium nanoparticles which was released due to possible leaching during the reaction process. Based on UV-Visible absorption spectroscopy and powder XRD we conclude that, there was no reaction between CdSe/PPy and $PbCl_2$ at room temperature thus limiting its scope to only mercury ions. Therefore, it can be summarized that, CdSe/PPy and Se/PPy are specific to detection of mercury ions at ppm level.

3. Experimental

3.1 Materials and methods

Cadmium acetate dihydrate, Selenium dioxide, Pyrrole, Mercury (II) chloride were purchased from Sigma Aldrich India Ltd., Chloroform ($CHCl_3$), Methanol (CH_3OH) and N, N'-dimethyl formamide (DMF) were purchased from Merck Chemicals India Ltd., Lead dichloride was purchased from Alfa-Aesar India Ltd. and were used as received. All solvents were used without any further purification.

UV-Visible absorption spectrum of CdSe/PPy and Se/PPy were obtained after re-dispersing the sample in DMF through ultrasonic irradiation. Photoluminescence (PL) spectra were obtained on Cary-Eclipse Fluorescence spectrophotometer of Agilent Technology at an excitation wavelength of 450 and 430 nm. FTIR spectroscopic measurements were taken on Perkin Elmer Spectrum Two. Thermal stability and enthalpy change of nanocomposites was determined in the range of room temperature to 800°C at a heating rate of 10°C/min under nitrogen atmosphere by thermo-gravimetric analysis (TGA) and differential thermal analyser (DTA) on a Perkin Elmer STA 6000 (simultaneous Thermal Analyser). The particle size distribution of dispersed nanocomposites was measured using NANOPHOX (SYMPA) based on the principle of photo-correlation spectroscopy using Laser beams. Morphology of the samples was studied by Scanning Electron Microscopy (SEM) and composition by Energy Dispersive Spectrometer (EDS) on JEOL/JSM-6360A. Transmission Electron Microscopy (TEM) was recorded on TECNAI G2-20-TWIN, FEI. X-ray Diffraction patterns were collected on a (Cu-Kα; λ=1.5406 A^0) radiation on Mini Rigaku X-ray Diffractometer. The microwave synthesis was performed in CEM Discover microwave synthesizer model no. 908010 (frequency 2455 MHz, Power 300W). To measure the electric properties broadband dielectric studies of the samples were performed using a dielectric spectrometer (Novocontrol Alpha-A) analyzer. The measurements were carried at 1000 Hz frequency and over a temperature range of (-) 25 to (+) 90°C. The samples were made into pellets (13 mm diameter) and proper electric contact was made with a silver paste and placed between gold platted electrodes for electrical measurements.

3.2 Synthesis by chemical method

Synthesis of CdSe/PPy (a)

In an open beaker, $CdAc_2.2H_2O$ (1.0gm), SeO_2 (0.4gm), and Pyrrole (5 mL) were stirred at room temperature for 2h, by which time blackish suspension was formed which was heated for 30 minutes at 70^0-80^0C. The mixture was centrifuged at 5000 rpm for 30 min giving rise to black precipitate which was washed with water followed by methanol. So-obtained black precipitate was dried in vacuum oven at 55^0C. The yield of the finally dried black powder was > 80%.

Synthesis of Se/PPy (b)

In a typical procedure, selenium dioxide (SeO_2) (1.0gm) and Pyrrole (5 mL) were mixed at room temperature with gentle stirring. The mixture was allowed to stir for 2-3 hrs, the resultant black coloured solution was then centrifuged at 5000 rpm for 30 min and black precipitate was washed with water and methanol several times. Washing with chloroform was given to remove excess pyrrole. Finally so-obtained precipitate was dried in vacuum oven at 55^0C for 3 h. The yield of the dried black powder was > 90%.

CdSe/PPy *via* Se/PPy precursor route (c)

In an open beaker, 1.0 gm of $CdAc_2.2H_2O$, 0.3 gm of Se/PPy precursor and 5 mL of Pyrrole, was stirred together at room temperature for about 2 hours. The reaction mixture was heated thermally for an hour at 70^0-80^0C to obtain a black powder. So-obtained powder was washed with water and centrifuged at 5000 rpm for 30 min followed by further washing with methanol. The yield of the dried powder was > 85%.

3.3 Synthesis by Microwave method

Synthesis of CdSe/PPy (d)

A mixture of pyrrole (5ml), cadmium acetate dihydrate (1.0gm) and selenium dioxide (0.4gm) was irradiated in a 50ml microwave synthesizer glass tube with 150 Watts power of microwave radiation for 15 min at 100°C in closed condition. The resulted black precipitate was worked up as described in procedure for synthesis of CdSe/PPy by chemical method (above) to get black powder in ~ 90% yield.

Synthesis of Se/PPy (e)

A 50ml microwave synthesizer tube containing mixture of pyrrole (5mL) and selenium dioxide (1.0gm), was irradiated with 150 Watts power of microwave radiation for 10 min at temperature 100°C in closed condition. The resultant black colored mixture was subjected to centrifugation at 6000 rpm for 15 min to obtain a black powder which was washed twice with methanol (30ml) and water (40ml). The obtained powder was dried under vacuum at 50°C for 2-3 hours. Yield of the dried black powder was ~ 85%.

4. Conclusions

We have described a simple one-step *(in-situ)* synthesis of CdSe/PPy and Se/PPy nanocomposite where selenium precursor acts as an internal oxidising agent and initiator for polymerisation of pyrrole. The reduction of cadmium and selenium ions by pyrrole followed by conversion to nanoparticles leads to the formation of CdSe/PPy and Se/PPy nanocomposites. As-synthesized nanocomposites were characterised thoroughly by using UV-visible, FTIR, Raman spectroscopy, SEM/EDAX, TEM analysis and powder XRD measurements. The results obtained indicated formation of CdSe and Se nanoparticles in PPy matrix. SEM revealed presence of smaller particles as clustered globules with smooth surface of CdSe/PPy and Se/PPy. TEM showed spherical CdSe and Se nanoparticles with d-spacing of 0.35 and 0.4 nm respectively confirming formation of nanoparticles. Impedance analysis showed gradual increase in conductivity for CdSe/PPy with temperature due to charge transfer properties while almost constant conductivity observed in case of Se/PPy nanocomposite. The CdSe/PPy and Se/PPy so prepared have been tested for detection of Hg^{2+} ions by UV-Visible spectroscopy. CdSe/PPy and Se/PPy nanocomposite showed ability to detect mercury ions (25, 50 and 100 ppm) in aqueous solutions with possibility of formation of HgSe on the surface of the composite. The formation of HgSe could is assumed to be due to cation-exchange menchanism and/or the release of Se^{2-} ion from the backbone of PPy.

Acknowledgements

We thank Vice-chancellor DIAT for encouragement and support. SB and AK thank DIAT for fellowships. VD and PKK thank DST for financial support through grant no. SR/S1/PC-39/2010.

Notes and references

1 M. M. Ayad, *J. Mater. Sci.,* 2009, **44**, 6392-6397.
2 L. Jiwei, Q. Jingxia, Y. Miao and J. Chen, *J. Mater. Sci.,* 2008, **43**, 6285-6288.
3 W. Wang, R. Zhang and G. Shi, *J. Mater. Sci.,* 2009, **44**, 3002-3005.
4 H. S. O. Chan, M. Y. B. Teo, E. Khor and C. N. Lim, *J. Therm. Anal.,* 1989, **35**,765-774.
5 H. Ge, P. R. Teasdale and G. G. Wallace, *J. Chromatogr. A,* 1991, **544**, 305-316.
6 S. Sukeerthi and A. Q. Contractor, Indian J. Chem., 1994, **33A**, 565-571.
7 S. B. Adeloju, S. J. Show and G. G. Wallace, *Anal. Chim. Acta,* 1993, **281**, 611-627.
8 A. Diaz, and J. Bargon, *Handbook of Conducting Polymers, ed. T. A. Skotheim,* 1986, **1**, 82-100.
9 A. F. Diaz and K. K. Kanazawa, *Extended Linear Chain compounds, ed. J. S. Miller, New York,* 1982, **3**, 417-430.
10 E. T. Kang, Y. P. Ting, K. G. Neoh and K. L.Tan, *J. Chem. Technol. Biotechnol,* 1994, **59**, 31-36.
11 E. T. Kang, Y. P.Ting, K. G.Neoh and K. L. Tan, *Synth. Met.,* 1995, **69**, 477-478.
12 K. H. Kate, K. Singh and P. K. Khanna, *J. Synth. React. in Inorganic, Metal-Organic and Nano-Metal Chemistry,* 2011, **41(2)**, 199-202. Sunil K. Pillalamarri, Frank D. Blum, and Massimo F. Bertino *Polymer Preprints* 2005, **46(1)**, 483
13 H. Laborde, J. M. Leger and C. Lamy, *J. Appl. Electrochem.,* 1994, **24**, 219-226.
14 R. Gangopadhyay and A. De, *Chem. Mater.*, 2000, **12**, 608-622; F. Bensebaa, A. F. Abdiaziz, D. Wang, C. Bock, X. Du, J. Kung, and Y. L. Page, *J. Phys. Chem. B,* 2005, **109**, 15339-15344.
15 P. O. Esteban, J. M. Leger, C. Lamy, F. C. Garnier and A. Yassar, *J. Appl. Electrochem.*, 1990, **20**, 524-526.
16 I. Becerik and F. Kadirgan, *J. Electroanal. Chem.,* 1997, **436**,189-193.
17 I. Becerik, S. Suuzer and F. Kadrgan, *J. Electroanal. Chem.,* 1999, **476**, 171-176.
18 D. J. Strike, N. F. De Rooij, M. Koudelka-Hep, M. Ulmannand and J. Augustynski, *J. Appl. Electrochem.,* 1992, **22**, 922-926.
19 J. Zhang, X. Liu, L. Zhang, B. Cao and S. Wu, *Macromol. Rapid Commun.,* 2013, **34**, 528-532.
20 K. H. Kate, S. R. Damkale, P. K. Khanna and G. H. Jain, *J. Nanosci. Nanotechnol.*, 2011, **11**, 7863-7869.
21 Namrata Gaikwad, Sreenu Bhanoth, Priyesh V. More, G. H. Jain and P. K. Khanna, *Nanoscale*, 2014, **6**, 2746-2751; R. Liu, *Materials*, 2014, **7**, 2747-2771.
22 K. Murakoshi, R. Kogure, Y. Wada and S. Yanagida, *Solar Energy Materials and Solar cells,* 1998, **55**, 113-125.
23 Shumaila, M. Alam, A. M. Siddiqui and M. Husain, eXPRESS *Polymer Letters,* 2013, **7**, 723-732.
24 H. Dhyani, C. Dhand, B. D. Malhotra and P. Sen, *J Biosens Bioelectron,* 2011, **3**, 1-9.
25 J. D. Kehlbeck, M. E. Hagerman, B. D. Cohen, J. Eliseo, M. Fox, W. Hoek, D. Karlin, E. Leibner, E. Nagle, M. Nolan, I. Schaefer, A. Toney, M. Topka, R. Uluski, and C.Wood, *Langmuir,* 2008**,** ***24,*** 9727-9738.
26 E. Ozkazanc, S. Zor, H. Ozkazane and S. Gumus, *Polymer Engineering and Science,* 2013, **53**, 1131-1137.
27 E. D. Peterson, G. M. Smith, M. Fu, R. D. Adams, R. C. Coffin, and D. L. Carroll, *Appl. Phys. Lett.,* 2011, **99**, 073304-1-073304-3).
28 N. Singh, P. K. Khanna, Y. Patil, S. Lonkar, A. S. Reddy, and A. K. Viswanath, *Mater. Chem Phys,* 2006, **97**, 288-294.
29 P.K. Khanna and N.Singh, *J.Luminescence,* 2007,**174**,474-478.
30 P. Phukan and D. Saikia, *International journal of photoenergy*, 2013, **2013**, 1-6.
31 A. Ramanavicius, V. Mostovojus, A. Kausaite, I. Lapenaite, A. Finkelsteinas and A. Ramanaviciene, *Biologija*, 2006,**3**, 43-46.
32 H. Eisazadeh, *World Journal of Chemistry,* 2007, **2**, 67-74.

33 Y. Wang, G. A. Sotzing and R. A. Weiss *Chem. Mater.,* 2008, **20**, 2574-2582.
34 (a) Aditi Jadhav, Pawan K. Khanna *RSC Advances*, 2015, **5**, 44756-44763 (b) S. Bhanoth, Priyesh V. More, Aditi Jadhav and Pawan K. Khanna, *RSC Advances*, 2014, **4**, 17526-17532, (c) R.K.Beri, P.K.Khanna, *Cryst. Engg. Commn.* 2010, **12,** 2762-2768.
35 D. A. Blake, R. M.Jones, R. C. Blake II, A. R. Pavlov, I. A. Darwish and H. Yu, *Biosensors & Bioelectronics,* 2001, **16**, 799-809.
36 Y.Kim, R.C. Johnson and J.T.Hupp, *NanoLett.,*2001,**1**,165-167.
37 C. S. Wu, M. K. Khaing Oo, and X. Fan, *ACS NANO,* 2010**, 4,** 5897-5904.
38 X. Wang, Y. Shen , A. Xie and S. Chen, *Mater. Chem. Phys*, **140**, 2013, 487-492.
39 C. M. Willemse, K. Tlhomelang, N. Jahed, P. G. Baker and E. I. Iwuoha, *Sensors,* 2011, **11**, 3970-3987.
40 C.Yanhong, W. Bin, L. Hui and Z. Linjie, *IEEE*, 2010, 1-4.
41 R. A. Khaydarov, R. R. Khaydarov and O. Gapurova*, Water research,* 2010, **44**, 1927-1933; D-V. Brezoi, *J. Sci. and Arts*, 2010, **1**, 53-58.
42 S.Y. Lu and I-Hsin Lin, *J. Phys. Chem. B,* 2003, **107**, 6974-6978
43 U. Lee, J. Choi, N. Myung, Il-Ho Kim, C. R. N. Chenthamarakshan, R. Norma, de Tacconi, and K. Rajeshwar, *Bull. Korean Chem. Soc.,* 2008, **29**, 689-692.
44 M. M. Abdi, H. N. M. Ekramul Mahmud, L. C. Abdullah, A. Kassim, M. Zaki Ab. Rahman and J. L. Y. Chyi, *Chinese J. Polym. S*ci., 2012, **30**, 93–100.
45 Y. Wang, H. Yang, Z. Xia, Z. Tong and L. Zhou, *Bull. Korean Chem. Soc.,* 2011, **32**, 2316-2318.
46 G. Xi, K. Xiong, Q. Zhao, R. Zhang, H. Zhang, and Y. Qian, *Crystal Growth & Design,* 2006, **6**, 577-582.
47 S. Jing, S. Xing, L. Yu and C. Zhao, *Mater. Lett.,* 2007, **61**, 4528-4530.
48 A. Tian and G. Zerbi, *J. Chem. Phys.*, 1990, **92**, 3886-3891.
49 Dollish, Fateley and Bentley, *A Wiley-Interscience Publication*, *John Wiley and Sons*, *New York*, ISBN0-471-21769-7.
50 G. Han, J. Yuana, G. Shia and F. Wei, Thin *Solid Film*s, 2005, **474**, 64-69.
51 A. K. Sinha, A. K. Sasmal, S. K. Mehetor, M. Pradhanand and T. Pal, *Chem. Commun.,* 2014, **50**, 15733-15736.
52 S. Madakbas, E. Cakmakc, M. V. Kahraman and K. Esmer, *Chemical Papers,* 2013, **67**, 1048-1053.
53 Y. Patil and P. K. Khanna, *J. Synthesis and Reactivity in Inorganic, Metal-Organic and Nano-Metal Chemistry,* 2008, **38,** 518-523.
54 S. Suresh and C. Arunseshan, *Appl Nanosci.,* 2014, **4**,179-184.
55 A. Singh, Aditee Joshi, S. Samanta, A. K. Debnath, D. K. Aswal and S. K. Gupta, *Applied Physics Lett.,* 2009, **95**, 202106-1-6.
56 T. Fatima, T. Sankarappa, J. S. Ashwajeet and R. Ramanna, *International Journal of Innovative Science, Engineering & Technology*, 2015, **2**, 204-213.
57 H. Zhang, Y. Wang, X. Xiong, D. Bai, Y. *Mater. Letts,.* 2007, **61**, 1474.
58 J. Chen, Y. C. Gao, Z. B. Xu, G. H. Wu, Y. C. Chen, C. Q. Zhu, Anal. Chim. Acta 2006, **577**, 77.
59 Z. B. Shang, Y. Wang, W. Jin, *J. Talanta* 2009, **78**, 364.
60 A. Antanovich, A. Prudnikau, V. Gurin, and M. Artemyev *Chemical Physics,* 2015, **04**, 455-480.
61 V. G. Litovchenko, *Condensed Matter Physics*, 2004, **7**(1), 167-177.
62 A. I-leisselbarth, A. Eychmiiller, M. Giersig, A. Mews, H. J. Weller, *Phy. Chem.* 1993, **97**, 5333-5340.
63 L. Pauling, The Nature of the Chemical Bond, *Cornell Univ., USA, 3rd ed.,* 1960.